Supporting Information

Analyses of trajectory on-the-fly based on the global reaction route map

Takuro Tsutsumi,[a] Yu Harabuchi,[a,b] Yuriko Ono,[a] Satoshi Maeda,[a] and Tetsuya Taketsugu[a,*]

[a]Department of Chemistry, Faculty of Science, Hokkaido University, Sapporo 060-0810, Japan

[b]Precursory Research for Embryonic Science and Technology (PRESTO), Japan Science and Technology Agency (JST), Saitama 332-0012, Japan.

Figure S1 shows more detailed routes from VRT1/TS1-1b to MIN1 for cases of (F) ~ (K). In a case of (F), 73 trajectories reach $MIN1_{IRC}$ which is directly connected along the IRC from the latest TS1-1d, while 12 trajectories reach $MIN1_{bifur}$ which is the terminal of the next IRC connected *via* TS1-1b from $MIN1_{IRC}$. The branching rate for $MIN1_{bifur}/MIN1_{IRC}$ is 12/73 (~0.16). We can make a further analysis for the bifurcation routes of these 85 (= 73 + 12) trajectories, by distinguishing $VRT1_{IRC}$ and $VRT1_{bifur}$. There are four patterns of the routes: TS1-1d → $VRT1_{IRC}$ → $MIN1_{IRC}$ (72; IRC route), TS1-1d → $VRT1_{IRC}$ → $MIN1_{bifur}$ (8; bifurcation route), TS1-1d → $VRT1_{bifur}$ → $MIN1_{bifur}$ (4; IRC-jump route), TS1-1d → $VRT1_{bifur}$ → $MIN1_{IRC}$ (1; IRC-jump + bifurcation route). Then, the rate for bifurcation is 9/76 (~ 0.12) while the rate for IRC-jump is 5/80 (~ 0.06). In addition to 85 trajectories, one trajectory reaches $MIN1_{other}$ which is located on the next IRC in the other side of those with $MIN1_{IRC}$ and $MIN1_{bifur}$. $MIN1_{outside}$ indicates NPI isomers of MIN1 other than six MIN1's shown in Fig. 4, and no trajectory reach $MIN1_{outside}$ in a case of (F).

In the other cases, (G) ~ (K), trajectories approach transition states of the other IRCs before reaching MIN1. In a case of (G), 62 trajectories approach TS1-3a first, and then, they reach MIN1 ($MIN1_{IRC}$: $MIN1_{bifur}$: $MIN1_{other}$: $MIN1_{outside}$ = 46 : 13 : 0 : 3). This large number of trajectories can be understood by considering the similarity of geometry between VRT1/TS1-1b and TS1-3a (d = 15.9 Å $amu^{1/2}$) (see Fig. 2). Among 62 trajectories, 51 trajectories go directly to MIN1, while 7, 3 and 1 trajectories approach VRT1/TS1-1b, TS1-1a, and TS1-2, respectively, before reaching MIN1. In a case of (H), 22 trajectories approach to $TS1\text{-}1d_{outside}$ located in the outside of the local region shown in Fig. 4 where the tringle of the bottom of Au_5 in $TS1\text{-}1d_{outside}$ is inverted from those in TS1-1d, TS1-1d', and TS1-1d''. As shown in Fig. 9 (H), seven trajectories do not reach

MIN1 during 3 ps. As for the branching rate of the arrival MIN1, $MIN1_{IRC}$: $MIN1_{bifur}$: $MIN1_{other}$: $MIN1_{outside}$ = 12 : 3 : 0 : 0. In other cases of (I), (J), and (K), the trajectories first approach to other TSs, TS1-1a, TS1-2, and TS1-4, respectively, before reaching MIN1.

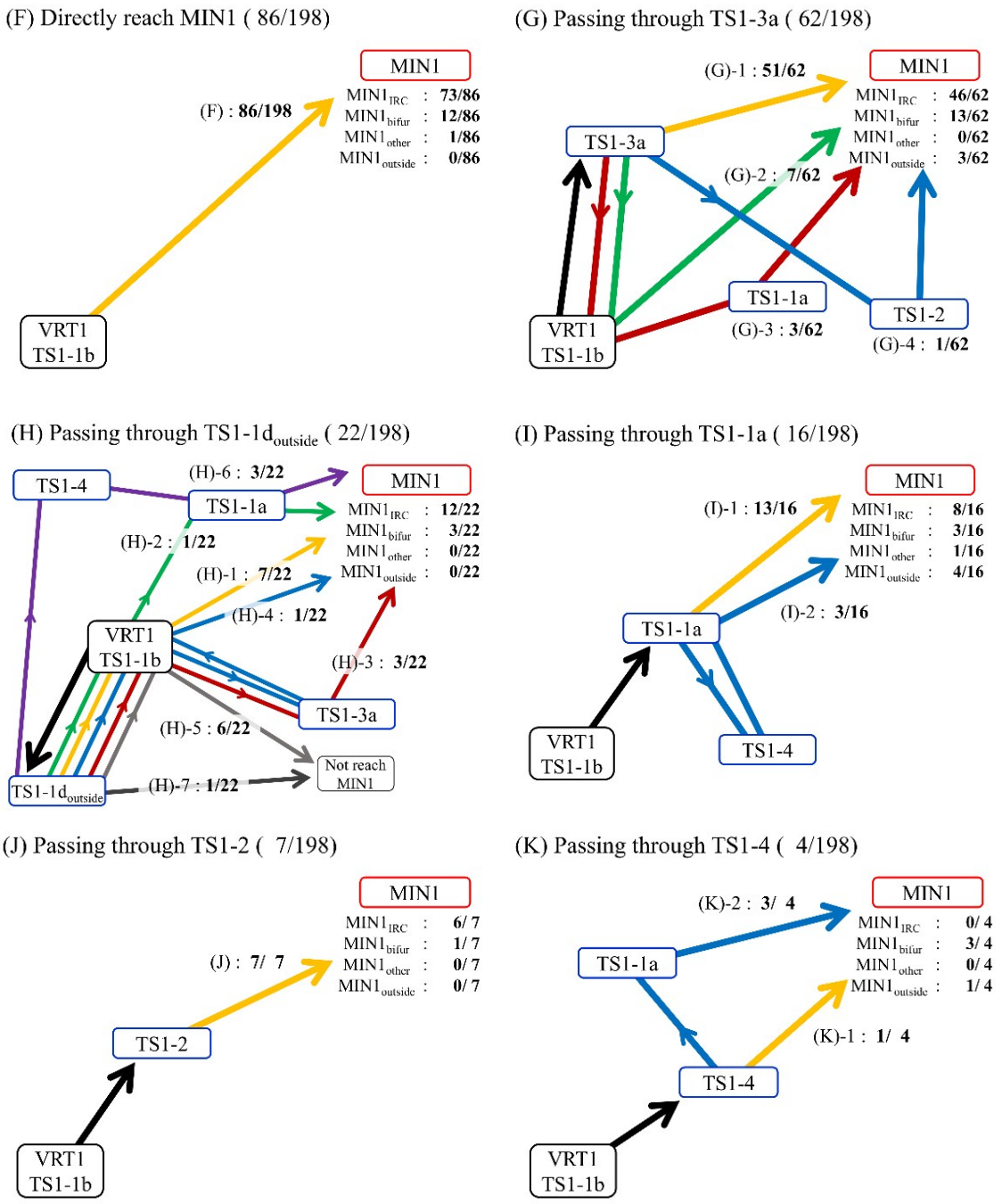

Figure S1. Schematic pictures for the AIMD routes from TS1-1d to MIN1 in cases of (F), (G), (H), (I), (J), and (K).